NASA CONTRACTOR REPORT 166610

A Study of Flow Past an Airfoil with a Jet Issuing from its Lower Surface

A. Krothapalli
D. Leopold

CONTRACT NAG 2-111
and NCC 2-198

June 1984

NASA

NASA CONTRACTOR REPORT 166610

A Study of Flow Past an Airfoil with a Jet Issuing from its Lower Surface

A. Krothapalli
D. Leopold

Prepared for
Ames Research Center
under Grant NAG 2-111
and Cooperative Agreement NCC 2-198

National Aeronautics and
Space Administration

Ames Research Center
Moffett Field, California 94035

ABSTRACT

An experimental investigation was conducted to study the aerodynamics of a NACA 0018 airfoil with a rectangular jet of finite aspect ratio exiting from its lower surface at 90° to the chord. The jet was located at 50 percent of the wing chord. Measurements include static pressures on the airfoil surface, total pressures in the near wake, and local velocity vectors in different planes of the wake. These measurements were made at jet momentum coefficients ranging from 0 to 2. Results from these measurements were to study the effects of jet-cross flow interaction on the aerodynamics of the airfoil. Results indicate that at all values of momentum coefficients, the jet cross flow interaction produces a strong contrarotating vortex structure in the near wake. The flow behind the jet forms a closed recirculation region which extends up to a chord length down stream of the trailing edge. As a result of these, the flow field becomes highly three dimensional; thus, the various aerodynamic force coefficients vary significantly along the span of the wing. A comparison of these results with a jet flap configuration is also made.

ACKNOWLEDGEMENTS

Many in the Joint Institute of Aeronautics and Acoustics contributed in various ways in this research, and we would like to thank each for their help.

Mr. A. Gerner and Mr. D. Durston of NASA Ames Research Center provided us the seven hole cone probe along with necessary calibration procedures. Without their help, the three dimensional velocity measurements would have not been possible. Special thanks are due to Messers Jerry deWerk and Al Armes whose outstanding work on the model made this experiment possible. Mr. Dale Buremann assisted in the operation of much of the electronics. Our thanks to him. The interest of Mr. George Aoyagi and Mr. David Koenig of NASA Ames Research Center in this work is greatly appreciated.

LIST OF SYMBOLS

AR	Nozzle aspect ratio
b	Span of the airfoil
C	Chord of the airfoil
C_d	Pressure drag coefficient; $d/q_\infty C$
C_l	Sectional lift coefficients; $l/q_\infty C$
C_m	Momentum coefficient; $M/q_\infty C$
C_p	Pressure coefficient; $(p - p_\infty)/q_\infty$
D	Width of the nozzle exit
d	Induced pressure drag
J	Momentum of the jet per unit span; $\rho_j\ U_j^2 D/C$
l	Induced sectional lift; $\int C_p d(x/c)$
M	Pitching momentum about the leading edge; $\int C_p\left(\frac{x}{c}\right) d\ (x/c)$
p	Surface presure on the airfoil
p_∞	Free stream pressure
ρ	Density
q_∞	Free stream dynamic pressure; $\frac{1}{2}\rho_\infty U_\infty^2$
Re_∞	Reynolds number of the free stream; $\frac{U_\infty C}{\nu_\infty}$
Re_j	Reynolds number of the jet; $\frac{U_j D}{\nu_j}$
U_j	Mean velocity at the center of the nozzle exit
U_∞	Free stream mean velocity
ν	Kinematic viscosity
α	Geometric angle of attack

TABLE OF CONTENTS

1. INTRODUCTION

During the past several years there has been an increased interest in V/STOL aircraft confiurations which utilize lift jets and thrust augmentors mounted in wings and/or the fuselage. One such configuration of interest uses a high lift system consisting of a wing with a long rectangular jet along the span issuing from below. Such a jet could be produced by installing two dimensional ejectors along the span of the wing. While these configurations usually exhibit improved lift characteristics, the interaction of the jet and the free stream can result in undesirable aerodynamic loading characteristics influencing the aircraft performance. For example, in hovering entrainment of the surrounding air by the jet induces a suction pressure on the lower surface of the wing causing a downward or suck down force. Close to the ground this load can be considerably larger. During transition from hovering to conventional forward flight this interaction produces a region of positive pressure upstream of the jet and a region of negative pressure downstream of the jet resulting, under certain conditions, in a net loss of lift and nose up moment. The extent of these regions depend on various parameters governing the flow field, such as the velocity ratio (jet exit velocity/free stream velocity).

Various aspects of the jet induced effects on wings and fuselages have been the subject of many studies; and most of these have been experimental investigations. Currently, in most V/STOL aircraft designs a semi-empirical approach guided by experimental data is employed to model the specific jet induced flow field. Several researchers, over the years, have surveyed and described these propulsive or jet induced effects (Margason[1], Skifstad[2]). More recently Kuhn[3] gave a comprehensive account of the induced aerodynamics of jet and fan powered aricraft. And recent advances in prediction methods for these effects on V/STOL aircraft was given by Agarwal[4]. Since these reviews are quite extensive, no attempt is made here to discuss the previous work on jet induced aerodynamics.

Experiments involving simple geometries, such as an axisymmetric jet issuing from an

airfoil or a flat plate have been carried out by several investigators. Most of the references related to these experiments were compiled by Perkins and Mendenhall[5]. In addition, they developed a correlation method to predict the surface pressure distribution on an infinite flat plate from which a jet is issuing. Yen[6] examined the experimental and analytical results on the aerodynamics of a jet in a cross flow. More recently Fearn[7] reported the progress towards a model to describe jet aerodynamics-surface interaction effects. In all these studies and the references cited there in, the jet exit in most cases has a circular cross section. Few studies[8,9,10] have also been carried out to study the influence of the nozzle exit cross section on the jet induced effects, using rectangular nozzles of aspect ratios less than five. Although the measurements reported in the previous works have contributed significantly to the present understanding of the jet-cross flow problem, with a particular emphasis on axisymmetric jets, there seems to be a need for a basic study of the jet-induced effects resulting from the interaction of two dimensional jet (or high aspect ratio rectangular jet) with the cross stream. In particular, the effect of this interaction on the regions upstream and downstream of the jet. To address this problem, Krothapalli et. al.[11] studied the aerodynamics of an airfoil with a jet exhausting from its lower surface. This experimental study was mainly exploratory in nature, and was not complete enough to provide any detailed understanding of the complex flow development of the jet and the flow around the airfoil. However, it provided a basis for the present study. Also, a theoretical analysis of the aerodynamics of an airfoil with a two dimensional jet issuing from its lower surface was carried out by Tavella and Karamcheti[12]. Their results were used here to compare with the present experimental data.

The purpose of this investigation is to study exprimentally the aerodynamic properties of an airfoil with a high aspect ratio rectangular jet, placed along the span, exiting from its lower surface. The airfoil used is the NACA 0018; with the nozzle located at mid chord as shown in figure 1.

2. NATURE OF THE PROBLEM

The problem concerned here is the determination of the various aerodynamic forces of the airfoil resulting from a jet issuing normal to its chord line into a uniform cross flow as shown in figure 1. The interaction between the jet and the cross flow in the presence of an airfoil is characterized by the following parameters: the goemetry of the airfoil, angle of attack of the airfoil, free stream velocity, free stream Reynolds number based on the chord of the airfoil, the geometric parameters of the nozzle, location and orientation of the jet with respect to the airfoil, velocity or Mach number of the jet, and the nature of the conditions at the nozzle exit and the free stream.

The main interest here is the determination of the forces on the airfoil and the flow field surrounding it. Such a determination and examination of how it varies with various parameters require a clear understanding of not only the jet structure but also the flow field around the airfoil due to the presence of the jet at different conditions of the parameters.

The goal of the experimental program is to understand the main physical features of such a flow and obtain satisfactory relations between the flow characteristics and the many parameters governing them.

The airfoil used was the NACA 0018. An aspect ratio of 407 was selected for the nozzle and oriented with its short edges parallel to the stream. The nozzle was located at 50 percent of the chord. The inlet section of the nozzle was designed such that the jet exits normal to the chord. For most measurements the free stream velocity was kept constant at 20 m/sec. The corresponding Reynolds number $R_e = \frac{U_\infty C}{\nu}$, is 2×10^5. The mean velocity at the nozzle exit was varied from 20 m/sec to 250 m/sec. The angle of attack of the airfoil was varied from $-10°$ to $15°$.

3. APPARATUS, INSTRUMENTATION AND PROCEDURES

The experimental study was aimed at gaining some insight into the flow features associated with the jet-cross flow interaction and its influence on the overall aerodynamics of an airfoil. The work involved measuring the lift, drag and pitching moment coefficients of the airfoil at different velocities of the jet, and different angles of attack of the airfoil. Also measured were some characteristics of the wake and the jet. The following sections describe the experimental set-up and the methodology using the course of this experiment.

3.1 WIND TUNNEL

The wind tunnel used in this experiment was a subsonic closed circuit type. The test section which was square cross-section has the dimensions of 90.2 × 45.7 × 45.7 cm. The flow speed in the test section can be varied between 20 m/sec and 65 m/sec.

The wind tunnel was run at a nominal speed of 20 m/sec. The model was situated midway between the upper and lower walls of the test section (see figures 2 and 3). The profiles of the mean velocity and the R.M.S. values of the velocity fluctuations in the empty test section were measured at different locations of the test section. The measurements show very uniform profiles, except very close to the walls. The free stream turbulence level was found out to be about 0.47 percent.

3.2 MODEL

A NACA 0018 symmetric airfoil was chosen for the experiment. The airfoil profile and its characteristics were given by Abbott et al[13]. The airfoil was made in several sections using aluminum and stainless steel . It has a 15cm chord and spans the entire 45.7cm length of the test section as shown in figure 2. The aspect ratio of the wing was equal to about 3.05. A rectangular slot with its long dimension perpendicular to the chord was cut into the lower surface at midchord. Two aspect ratios were used for the nozzle exit. The

first series of tests was run with a slot of aspect ratio 87. The length and width of the nozzle exit were 26cm amd 0.3cm respectively. Following these tests, a slot of an aspect ratio 407 was used. The long and short dimensions of this nozzle were 40.7cm and 0.1cm. Before air reaches the nozzle exit, it passes through a settling chamber which extends along the span of the wing. Compressed air was supplied to the settling from both ends of the wing (see figure 3). To ensure a uniform flow at the nozzle exit, adjustable vanes were placed inside the settling chamber. The inlet section of the slot was designed in such a manner that the jet stream exhausts perpendicular to the chord of the airfoil. With the optimum position of the vanes, a uniform flow was obtained. The variation of the mean velocity along the span was within ten percent of the value at the center of the nozzle exit.

3.3 MEASUREMENTS

Surface pressure measurements were made using 84 taps distributed chord wise on the upper and lower surfaces at both midspan and quarter span positions, and along spanwise locations on the lower surface at 80 percent of the chord; as shown in figure 4. These pressure taps were connected to a 96 port scanivalve unit using metal and tygon tubing. To obtain the wake and jet characteristics, a seven hole conical pressure probe was used. A detailed description of its theory and calibration was given by Everett et.al.[14]. This probe is capable of measuring flow conditions at angles up to 75° relative to its axis. Although this probe was designed to be used in high subsonic and supersonic flows, the calibration at low subsonic velocities revealed that it can also be used in the velocity range under consideration. In order to minimize the flow distrubances the probes were made quite small (about 0.25 cm in diameter). Calibration establishes polynomial expressions to represent the local angle of attack, angle of slide slip, total pressure and static pressure. When sampling an unknown flow, these flow quanties are computed directly from their corresponding polynomial expressions. The local total and static pressures are then used to calculate local velocity. Using this probe, measurements were made in several planes

as shown in figure 5. The seven hole probe and its mounting arrangement can be seen in figure 3. To aid in the visualization of the flow, a tuft survey was conducted in various parts of the flow field.

A PDP 11/23 mini computer was used to operate and control the scanivalve and the traversing mechanism; which was used to support the seven hole probe. The computer was also used to store and analyze the data.

3.4 PROCEDURES:

The experiment was carried out in two stages. During the first stage, tests were conducted with a jet exiting from a nozzle having an aspect ration of 87; at zero angle of attack of the airfoil. Following these tests, the aspect ratio of the nozzle was increased to 407 to minimize the end effects of the jet. In this case the jet extends about 89 percent of the span. Most of the detailed measurements were made for the case of a large aspect ratio jet.

The jet exit velocity was varied from 0 m/sec to 240 m/sec. The corresponding momentum coefficient, which is defined as

$$C_\mu = J/q_\infty,$$

where J is the momentum flux of the jet per unit span, and given by

$$J = \rho_j U_j^2 D/C,$$

was varied from 0 to 2. The jet exits normal to the chord line of the airfoil.

For most measurements the free stream velocity was kept constant at 20 m/sec. The

corresponding Reynolds number, based on the chord of the airfoil is equal to,

$$Re = \frac{U_\infty C}{\nu} = 2 \times 10^5$$

To minimize the influence of the Reynolds number on the state of the flow, the boundary layer at the leadig edge of the airfoil was tripped.

Surface pressure measurements were made at several velocity ratios (nozzle exit mean velocity/free stream mean velocity), and at different angles of attack. The angle of attack was varied from $-10°$ to $15°$. To obtain the aerodynamic force coefficients the surface pressure data was integrated around the airfoil at two spanwise locations. The lift due to the jet reaction is not included in the data.

A cartesian co-ordinate system (x, y, z) was used with x axis oriented along the center line of the wing section with its origin located at the leading edge as shown in figure 1.

For most of the measurements errors were estimated to be of the order of five percent.

3.5 WIND TUNNEL WALL CORRECTIONS

The testing of V/STOL models in wind tunnels present many problems that are very different from those encountered in testing of conventional type airfoils, where the testing techniques are relatively well understood[15]. V/STOL models such as the one tested have relatively large wake deflection angle and high energy which presents one of the most difficult problems that is encountered in wind tunnel testing. The primary work in wind tunnel wall effects and their corrections for V/STOL configurations was done by Heyson[16]. Studies covering the limits on the minimum speed V/STOL wind tunnel test was done by Rae[17]. Recently Margason and Hoad[18] gave an account of V/STOL aircraft model in wind tunnel testing from model design to data reduction. In most of the instances the

model used is a fan-in-wing configuration. Since these correction techniques are highly configuration dependent, and the present wing model is not representative of any flight vehicle, no attempt is made here to correct the data.

One particularly important aspect of V/STOL model testing is the need to describe a "jet-off reference configuration" for each jet-on configuration tested. These data are then used to provide a basis for determining the interference of the jets on aerodynamic characteristics. Such a procedure was used in this experiment.

Another factor to take into account is the flow impingement on the test section floor. In a wind tunnel with the air moving with respect to the model and to the ground plane, there is a boundary layer on the floor. Jet exhausting from the model can impinge on the floor at appropriate test conditions and the flow forward of, and under, the model effects the overall flow field significantly. This problem can be minimized by using a moving belt ground plane. Several investigations have been carried out on this subject by Hackett et. al[19]. In the present case, because of the relatively small width (D = 3mm) of the nozzle exit and large distance from the jet exit plane to the wind tunnel wall (76D), wall effects caused by separation of the test section boundary layer due to jet impingement were small. And, as will be seen later, the jet in most cases does not reach the wall of the wind tunnel.

4. RESULTS AND DISCUSSION

A typical variation of the surface pressure on both upper and lower surfaces of the airfoil, at zero angle of attack with and without the jet, is shown in figure 6. The pressures are plotted in the form of the pressure coefficient C_p given by

$$C_p = (p - p_\infty)/q_\infty$$

It is observed that without the jet (i.e. $C_\mu = 0$), the pressure distribution on both sides of the airfoil are very nearly identical, confirming the symmetric property of the airfoil. For a relatively low momentum coefficient of 0.48, the influence of the jet on the surface pressure is quite significant as shown in the figure. When comparing this distribution with the jet-off condition the following observations are made: on the lower surface, in the region forward of the jet, and increase in pressure occurs, while a decrease in pressure is noticed in the region behind the jet. The positive pressure ahead of the jet is a result of the blockage of the free stream by the jet. The effect of this is an increase in effective angle of attack of the airfoil, thus resulting relatively low pressure on the upper surface of the airfoil. At a very low momentum coefficients the recirculation zone behind the jet is small and the flow reattaches to the lower surface. As the jet strength is increased by increasing the exit velocity, the flow in the region between the jet and the trailing edge forms a recirculation region and it extends into the wake. The magnitude of the pressure coefficient in this region was observed to be fairly constant as depicted by it's distribution in the region between the jet and the trailing edge in figure 6. The "Kutta Condition" requires that the pressure on both lower and upper surfaces at the trailing edge be equal. This being the case, the pressure on the upper surface near the trailing edge is fixed by its value in the recirculation region on the lower surface. It is interesting to note that very little variation in the magnitude of C_p is observed on the upper surface for x/c greater than about 0.6,

thus suggesting that only the pressure changes in the first half ($x/c < 0.5$) of the airfoil are mostly responsible for the generation of the induced lift. From these observations it may be suggested that the positive and negative pressure regions on the lower surface are essentially responsible for many changes in the gross aerodynamic characteristics of the airfoil to be noted later.

To minimize the effects of free stream Reynolds number on the surface pressure distribution, the surface near the leading edge was roughened using glass beads (4mm diameter) over a surface length of about 0.07c. To ensure this, a comparison of the pressure distributions at mid-chord for $C_\mu = 0.22$, at two different free stream velocities, is made in figure 7. Within the experimental error, it is observed that the two distributions are quite similar.

It has been known (see for E. G. Wooler et.al[20]) that the jet-cross flow interaction produces a highly three dimensional flow field which induces nonuniform pressure on the surface from which the jet is issuing. Keeping this in miud, the surface pressure distribution at the quarter span location of the airfoil was measured and is shown in figure 8, along with the corresponding midspan distribution for a $C_\mu = 0.54$. The difference between the two distributions is primarily concentrated on the lower surface, in the region between the jet and the trailing edge, in which a relatively large negative pressure occurs. In contrast to the midspan distribution, where the pressure for the latter half ($x/c > 0.5$) of the airfoil contributes very little to the lift force, at quarter span the distribution results in a force whose direction is opposite to that of the lift. As will be seen later that this negative interference lift force is a result of the flow induced by large scale vortices produced by the jet-cross flow interaction. although some changes are observed in the pressure distribution forward of the jet both on the lower and uper surfaces, they are relatively small.

To study the variation of the surface pressure with angle of attack, exepriments were conducted for several combinations of C_μ and α, and two typical plots of C_p vs x/c are shown in figures 9 and 10. Here, α is the geometric angle of attack. When the jet is on,

the effecti.e angle of attack, (i.e. the angle felt by the airfoil) will be greater than α. On comparing the two pressure distributions at $\alpha = 0$ and $\alpha = 8°$ (less than α stall), it is observed that the pressure distribution for the leading half of the airfoil show significant changes with varying angle of attack. These changes are quite similar to those observed for airfoils without the jet. However, when the angle of attack is greater than or equal to α stall, which also depends on the strength of the jet (i.e., C_μ), a significant increase in the pressure on the entire upper surface is observed as shown in figure 10. Also noticed is that the magnitude of the pressure for most of the leading half ($0.1 < X/C < 0.5$) of the airfoil on the upper surface is fairly constant, indicating flow separation. It is to be noted that the effective stall angle will be much greater than the geometric stall angle (α stall).

The extent of the influence of the momentum coefficient C_μ, on the regions (i.e. positive and negative pressures on the lower surface) described earlier can be characterized by the variation of the magnitudes of the C_p at two typical locations in front of (x/c = 0.47) and behind (x/c = 0.53) the jet with C_μ. This is shown in figure 11. For $C_\mu > 0.1$, the variation of C_p, at both locations, is monotonic and reaches a constant value at about $C_\mu = 1.0$. For greater than one, not shown here, very little change in their magnitudes is noticed.

Figure 12 shows the variation of the pressure along the span of the airfoil behind the jet at a chord wise location x/c = 0.8, for different values of C_μ. Without the presence of the jet (i.e. $C_\mu = 0$), very little variation if C_p along the span is observed; indicating the flow is two dimensional. When the jet is present, two distinct negative pressure regions on either side of the mid span location are seen in the figure. Corresponding to each of these regions is a large negative peak for the value C_p, which increases with increasing C_μ. This type of variation in C_p along the span generally reflects the presence of large vortices. As will be shown later from the seven hole probe data, that such vortices are present in this case. When the aspect ratio of the nozzle is reduced, these vortices will influence the surface pressure at the mid span of the wing and results in a lower sectional lift coefficient.

From the chordwise pressure distribution determined, the sectional lift was easily obtained by numerical integration of pressure over the span wise section. For each value of C_μ in the range tested, a corresponding sectional lift coefficient C_l was obtained at both mid span and quarter span locations. The reaction force due to the jet is not included in the definition of the lift. Figure 13 shows the variation of C_l with C_μ at both locations, and for $\alpha = 0°$. It can be seen that for both positions the magnitude of the C_l increases with increasing C_μ. However, the rate of increase (or slope) becomes smaller for C_μ greater than about 1.0. At a corresponding C_μ, the magnitude of C_l at quarter span is lower than that for the mid span. It is suggested that the lower sectional C_l at quarter span is due to the presence of the large scale vortices which are generated by the jet-cross flow interaction. The geometric position and the extent of their influence on the wing surface pressure depends, besides on the magnitude of C_μ, strongly on the aspect ratio of the nozzle. For example when the aspect of the nozzle is reduced, the influence of the vortices is even felt at the mid span of the wing as shown in Figure 14, which shows the variation of the sectional (mid span) lift coefficient with C_μ for two different aspect ratios of the nozzle. Also included in the figure is a theoretical curve obtained from an analysis developed by Tavella and Karamcheti[12]. In this analysis, the airfoil jet wake problem is introduced as a two dimensional inviscid flow boundary value problem where the wake is assumed to consist of a dead-air region at constant pressure equal to the pressure at infinity, and the jet is assumed to be infinitely thin. No entrainment effects are included. Despite the various simplifications built into the theory, it predicts reasonably well variation of C_l with C_μ. It is to be noted that when the jet spans the entire wing, the sectional C_l is generally found to be constant for all the locations along the span, for example, such an observation can be made in the studies of jet flaps.

In view of the observations made from figure 6 that only the leading half of the airfoil contributes to the lift, a comparison of the variation of the sectional C_l at mid span for

the leading half and full airfoil, with C_μ is shown in figure 15. For the range of C_μ tested it is observed that a significant portion (about 90 percent) of the total lift is contributed by the leading half of the airfoil.

In an attempt to compare the present results with a jet-flap configuration and in light of above discussion, the present airfoil may be replaced with a configuration as shown schematically in figure 16. Figure 17 shows the variation of the total lift with C_μ for the configuration shown in figure 16. The total lift of the airfoil is equal to the sum of the induced lift and vertical reaction to the jet thrust. Included in the figure is the data taken from a typical jet-flap study of Bevilaqua et. al[21]. In their study, the airfoil model has a thickness to chord ratio of 0.2 and was symmetrical except in the area of the blowing slot and the upper flap contour. The jet blowing slot was located on the upper surface at x/c = 0.9 and extends the entire span of wing. Using a flap surface, the jet deflection was set at 90° relative to the airfoil chord. Despite the differences in the geometries of the configurations, the overall trends of the data are quite similar. However, when compared at corresponding C_μ, the magnitude of C_l for the present configuration is lower than that of the jet-flap. The additional lift for the jet-flap configuration can be attributed to the boundary layer control provided by the jet on the upper surface of the airfoil.

The variation of the midspan C_l with C_μ for different values of the angles of attack α, is presented in figure 18. Except for the occurance of stall for $\alpha = 10°$, the overall behavior of the curves is quite similar. At corresponding values of C_μ, the magnitude of C_l increases with increasing α. To present the data in a more conventional manner, the C_l is plotted against the angle of attack for different values of C_μ in figure 19. Before stall, a linear variation of C_l with incidence, is observed. similar behavior was also noticed in many of the jet-flap investigations (e.g. Spence[22]). The lift curve slope for the case $C_\mu = 0$ was found to be about 1.5π, and does not change with increasing C_μ. This slope is lower than the theoretical value 2π for symmetrical airfoil without the jet.

From the integration of the streamwise component of the pressure around the airfoil, a drag force, known as pressure or form drag, is obtained. Figure 20 shows the variation of the sectional drag coefficient C_d with C_μ at both midspan and quarter span locations and for $\alpha = 0°$. As noted earlier, the quarter span location is influenced strongly by the presence of large scale vortices and, as a result, an increase in sectional drag as compared to the mid span location, is observed. The magnitude of C_d increases sharply for small values of C_μ and reaches a maximum value of $C_\mu = 0.6$. It then decreases gradually as shown in the figure. The effect of angle of attack on mid span drag coefficient is shown in figure 21. For the conditions tested except for the case of $\alpha = 8°$, the overall behavior of C_d with C_μ is quite similar. For $\alpha = 8°$, the magnitude C_d decreases with increasing C_μ until it reaches a minimum at $C_\mu = 0.6$, and increases sharply for $C_\mu > 0.6$. It may be suggested that for $C_\mu > 0.6$, separation occurs on the upper surface of the airfoil. A cross plot of the data in figure 21, in a more conventional manner, is shown in figure 22. For $C_\mu = 0$, the variation of the drag coefficient with α should be symmetric with respect to $\alpha = 0$. As shown in the figure, within limits of error for the experiment and the calculation of C_d, it appears that the variation of C_d is in agreement with the above observation.

Figure 23 shows the mid span moment coefficient about the leading edge of the airfoil with C_μ for different angles of attack of the airfoil. Here the negative values of C_m denotes the nose down moment. Except for the conditions of stall, magnitude of C_m seems to remain negative for all values C_μ. Similar nose down pitching moment was also observed[24] in a jet flap configuration.

In an attempt to study the flow structure in the wake of the airfoil, a seven hole conical pressure probe was used. The design and calibration of this probe was given by Everett et.al.[14]. This probe is capable of measuring flow conditions at angles up to 75° relative to its axis. From the pressure information obtained the magnitude and direction of the velocity was calculated. The following data was taken at $\alpha = 0°$. The next few figures

show the velocity vectors in different planes of the wake (see also figure 5). Because of the limited size of the test section, full vortex can be captured only at very low momentum coefficients of the jet. A typical plot of velocity vectors at a down stream location of x/c = 2.0, in the y-z plane; and for a nozzle of an aspect ratio of 86, is shown in figure 24. The flow field associated with the jet vortex, as well as the vortex location are readily apparent. Figures 25-27 show the velocity vectors in the yz plane (see also figure 5), for three different downstream locations starting at the trailing edge (i.e. x/c = 1.0). For all these cases the aspect ratio of the full nozzle was 407, and $C_\mu = 0.33$. Except for the wake of the airfoil the overall flow field clearly shows two distinct contratotating vortices located symmetirically on the either side of the midspan location. Similar vortex structure was also observed by Weston and Thames[8] in their investigation of a rectangular jet of aspect ratio four issuing into a subsonic cross flow. As noted earlier, the presence of these vortices influence significantly the overall aerodynamics of the airfoil.

In their theoretical formulation of this problem, Tavella and Karamcheti[12] asummed that the pressure in the wake, (i.e. the recirculation region between the jet and the lower boundary of the airfoil wake) be equal to the free stream pressure. This assumption causes the recirculation region to be open and infinite. However, in the present experiment, the pressure in this region was found to be much less than the free stream pressure, as indicated by the lower surface pressure in the region between the jet and the trailing edge (see for example figure 8). Generally, such a low pressure causes the recirculation region to be closed. Keeping this in mind, velocity vector measurements in the XY plane at two different span wise locations (z/c = 0, and z/c = 0.677) were made, and are shown in figures 28 and 29. These velocity vector plots suggest that the recirculation region ends at a down stream location of about x/c = 2. To study the extent of this region in XZ plane; measurements were made in a plane located below the trailing edge at y/c = 0.169. Again we observe that the recirculation zone extends up to x/c = 2.0. Outside of this region,

the velocity field seems to be quite symmetric and the orientation of the vectors are in agreement with the free stream direction. A data of this type shown in figures 25-30 give a quantitive picture of the three velocity components in different planes.

The downstream development of the mean total pressure profiles in the wake of the airfoil at zero of attack and for $C_\mu = 0.48$ is shown in figure 31. From these profiles one can observe the development of the wake (or recirculation region) and the jet with the down stream distance. The dotted lines shown in the picture represents the jet and wake center lines; which are drawn through the maximum and minimum pressures in each of the profiles.

From the wake total pressure profiles, the locus of points corresponding to the jet centerline can be obtained. These are plotted in figure 32, for two different values of C_μ. For comparison purposes the data for the jet-flap is included in the figure, which is taken from Bevilaqua et. al[21]. This data is for a jet issuing at 90° to the free stream at $C_\mu = 1.0$. The agreement between the two sets of data is satisfactory. It may be suggested from these observations, the development of the jet is not effected significantly by the presence of the recirculation region between the jet and the airfoil.

V. CONCLUSIONS

The following conclusions may be drawn from the current study:

The static pressure distribution around the airfoil shows two distinct regions on the lower surface, which greatly influence the overall aerodynamics. First there is the positive pressure region upstream of the jet. This is attributed to the "blockage" of the freestream by the jet. The second, is the region between the jet and the trailing edge, marked by the negative pressure coefficient, and the magnitude of the pressure coefficient in this region is found to be nearly constant. The pressure on the upper surface of the airfoil is also influenced by the presence of the jet, and the influence is such that only the pressure distribution for the leading half of the airfoil contributes to the lift coefficient. The increase in wing angle of attack α, resulted in an increase in the magnitude of the sectional lift coefficient C_l, for different values of the jet momentum coefficient C_μ. For less α than α stall, C_l varies linearly with α, quite similar to that of a jet-flap configuration.

Because of the finite aspect ratio of the nozzle, although quite large (AR = 407), the interaction of the freestream with the jet produces contrarotating vortex structure downstream of the trailing edge of the airfoil, quite similar to that observed in other jet-cross flow studies. The presence of these vortices significantly influence the spanwise pressure distribution, and the flow becomes highly three dimensional in nature. The extent of their influence on the overall flow field depends both on the aspect ratio of the nozzle and the velocity ratio (i.e. jet velocity/free stream velocity).

The flow behind the jet forms a recirculation region, which extends up to one chord length down stream of the trailing edge. The magnitude of the C_p with in this region was found to be constant and has negative value. The velocity vectors in this region suggest that the recirculation region is a closed one and the extent of which does not change significantly for $C_\mu > 1.0$. It appears that the development of the jet was not effected by

the presence of this recirculation or separated region of the flow.

REFERENCES

1. R. J. Margason; "Review of propulsion induced effects on aerodynamics of jet V/STOL aircraft", NASA TN D - 5617, 1970.
2. J. G. Skifstad; "Aerodynamics of jet pertinent to V/STOL aircraft", Journal of Aircraft, Vol. 7, No. 3, 1970.
3. R.E. Kuhn; "The induced aerodynamics of jet and fan powered V/STOL aircraft", Recent Advances in Aerodynamics, Edited by A. Krothapalli and C. A. Smith, Springer - Verlog, 1984.
4. R. K. Agarwal; "Recent advances in prediction methods for jet induced effects on V/STOL aircraft", Recent Advances in Aerodynamics, Edited by A. Krothapalli and C. A. Smith, Springer - Verlog, 1984.
5. S. C. Perkins Jr, and M. R. Mendenhall; "A correlation method to predict the surface pressure distribution on an infinite plate from which a jet is issuing", NEAR TR 160, Nielsen Engineering and Research Inc., 1978.
6. K. T. Yen; "The aerodynamics of a jet in a crossflow", NADC-78291 - 60, Naval Air Systems Command, 1978.
7. R. Fearn, "Progress towards a model to describe jet aerodynamics - surface interaction effects", Recent Advances in Aerodynamics, Edited by A. Krothapalli and C. A. Smith, Springer - Verlog, 1984.
8. R. P. Weston and F. C. Thames; "Properties of aspect - ratio - 4.0 rectangular jets in a subsonic cross flow", Journal of Aircraft, Vol. 16, No. 10, 1979.
9. J. C. Wu, H. M. McMahon, D. K. Mosher, and M. A. Wright; "Experimental and analytical investigations of jets exhausting into a deflecting stream", Journal of Aircraft, Vol. 7, No. 1, 1970.
10. D. L. Antani and H. M. McMahon; "Behavior of a subsonic turbulent slot jet in cross flow", Journal of Aircraft, Vol. 15, No. 12, 1978.
11. A Krothapalli, D. Leopold and D. Koenig; "An experimental investigation of flow surrounding an airfoil with a jet exhausting from the lower surface", NASA CR 166, 131, 1982.
12. D. A. Tavella and K. Karamcheti; "Aerodynamics of an airfoil with a jet issuing from its lower surface", AIAA Paper No. 82-0222, 1982.
13. H. J. Abbott and A. E. Van Doenhoff; "Theory of wing sections, Dover Publications, New York, 1949.
14. K. N. Everett, A. A. Gerner and D. A. Durston; "Theory and Calibration of Non-Nulling Seven-Hole Cone Probes for Use in Complex Flow Measurement", AIAA Paper No. 82-0232, 1982.
15. A. Pope and J. J. Harper; "Low speed wind tunnel testing", John Wiley & Sons Inc., 1966.
16. H. H. Heyson; "The effect of wind tunnel wall interference on the performance of a

fan-in-wing VTOL model", NASA TN D-7518, 1974.

17. W. H. Rae; "Limits on minimum speed V/STOL wind tunnel tests", Journal of Aircraft, Vol. 4, No. 3, 1967.
18. R. J. Margason and D. R. Hoad; "V/STOL aircraft model in wind tunnel testing from model design to data reduction", Vol. 17, No. 3, 1980.
19. E. J. Hackett and R. A. Bles; "Ground interaction and tunnel blockage for a jet-flapped, basic STOL model tested to very high lift coefficient", NASA CR - 137, 1976.
20. P. T. Wooler, G. H. Burghart and J. T. Gallagher; "Pressure distribution on a rectangular wing with a jet exhausting normally into an airstream", Journal of Aircraft, Vol. 4, No. 6, 1967.
21. P. M. Bevilaqua, P. E. Cole and E. F. Schum; "Progress towards a theory of jet flap thrust recovery", Rockwell International Report NR80H-70, 1980.
22. D. A. Spence; "The lift coefficient of a thin, jet-flapped wing", Proceedings of Royal Society A, Vol. 238, 1956.
23. J. Williams, S. F. J. Butler, and M. N. Wood; "The aerodynamics of jet flaps", ARC R & M 3304, 1961.
24. B. W. McCormick, Jr., Aerodynamics of V/STOL: flight, Chapter 7, Academic Press, 1967.

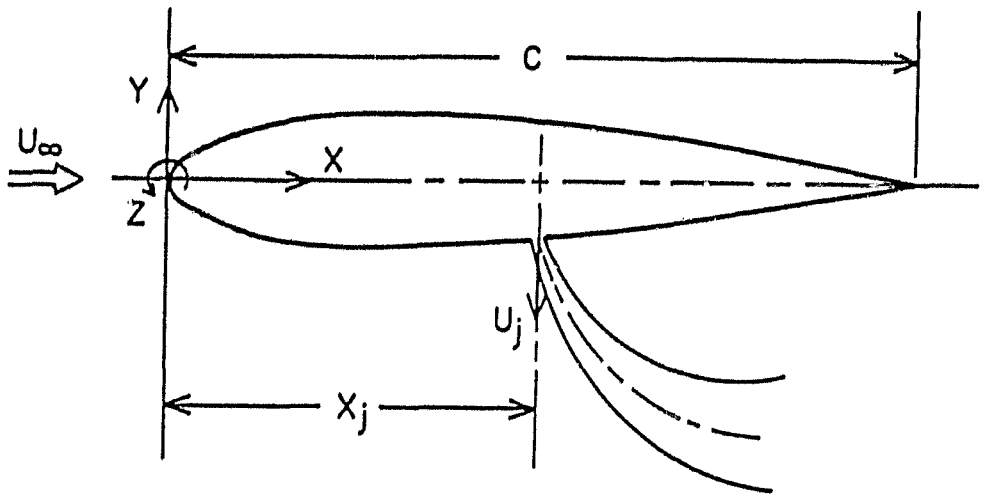

Figure 1. Definition sketch

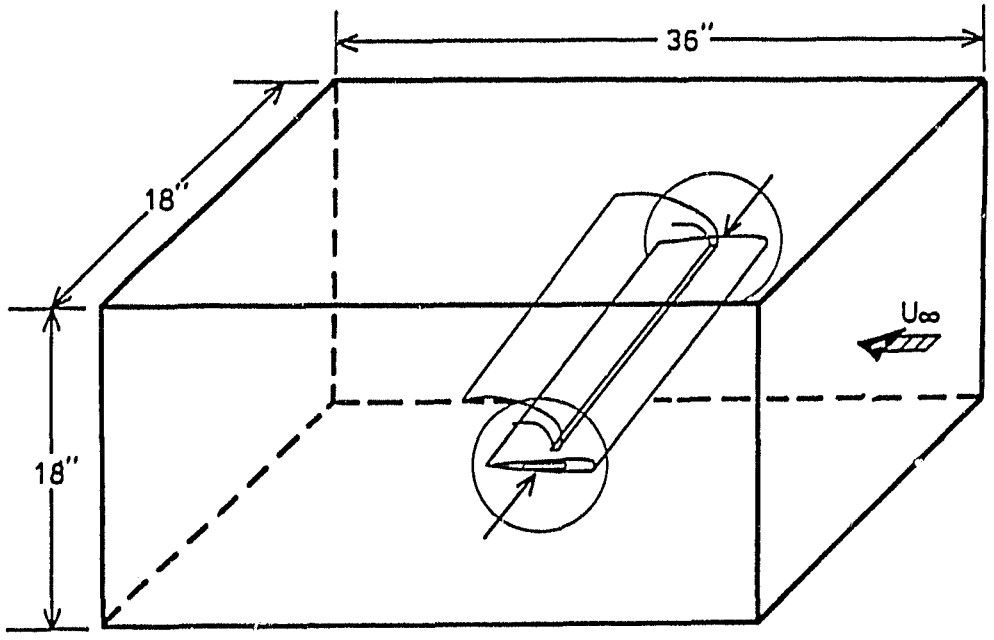

Figure 2. Arrangement of the model in the wind tunnel test section.

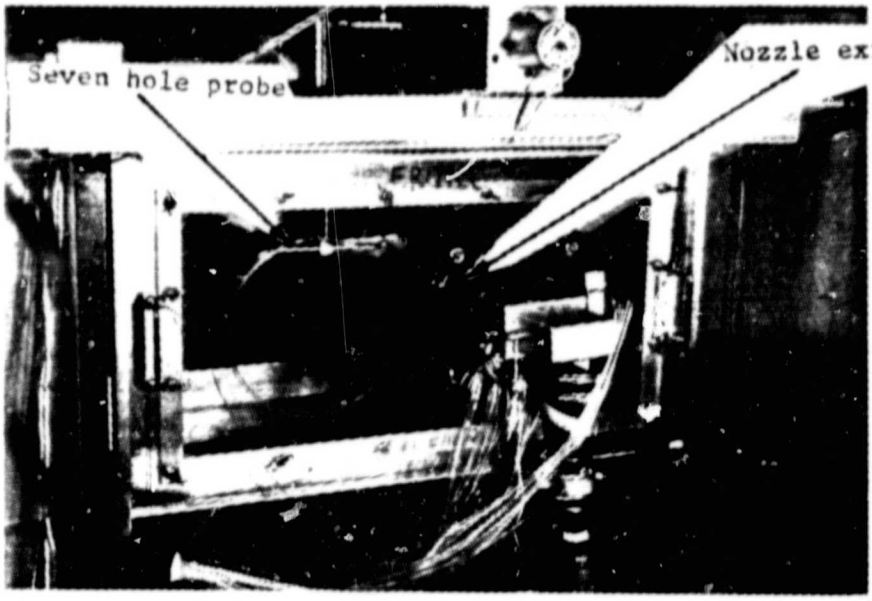

(a)

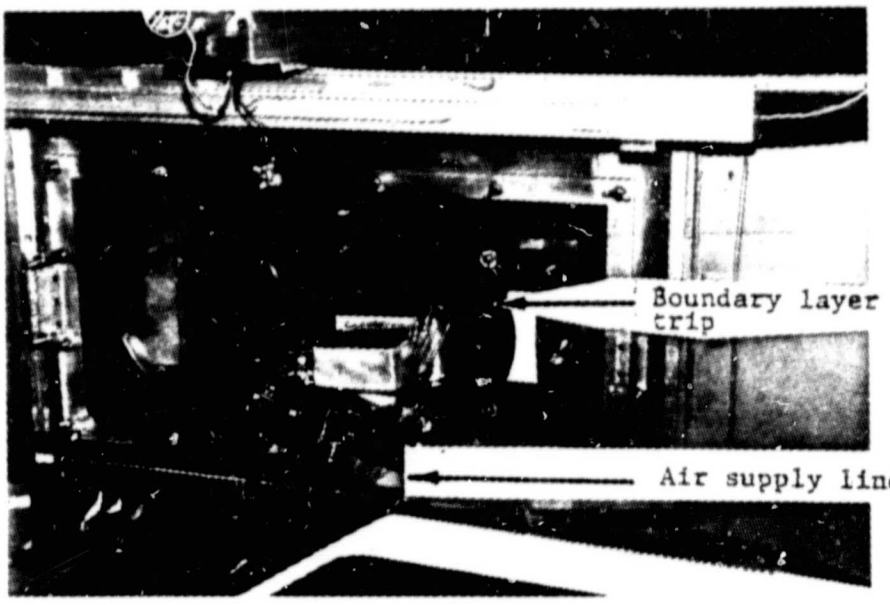

(b)

Figure 3. Photographs of the wind tunnel test section with the model in place

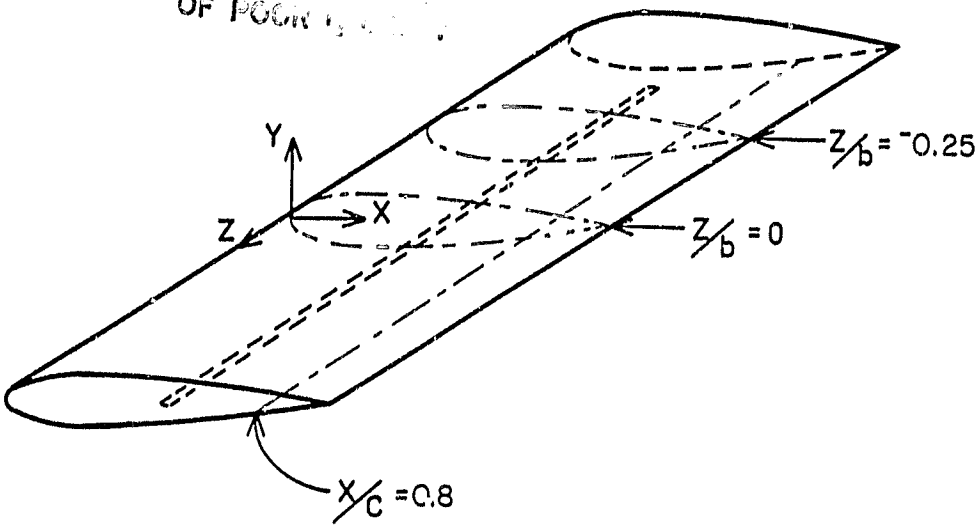

Figure 4. Locations of the static pressure taps.

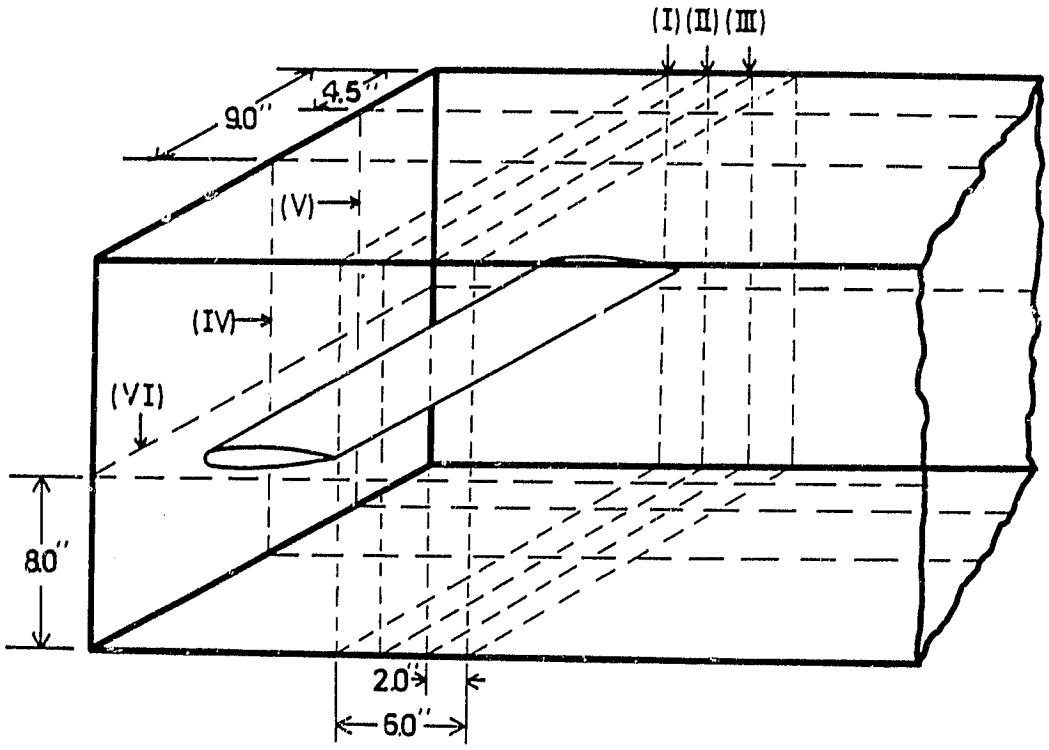

Figure 5. Locations of various planes for velocity vector measurements.

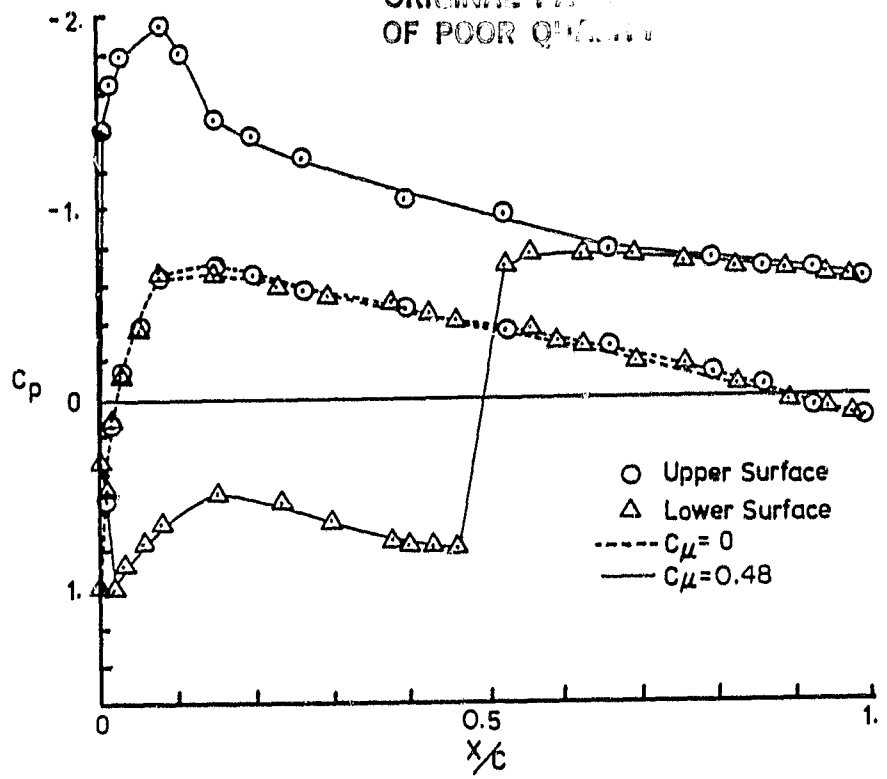

Figure 6. The distribution of the surface pressure on the airfoil at midspan.

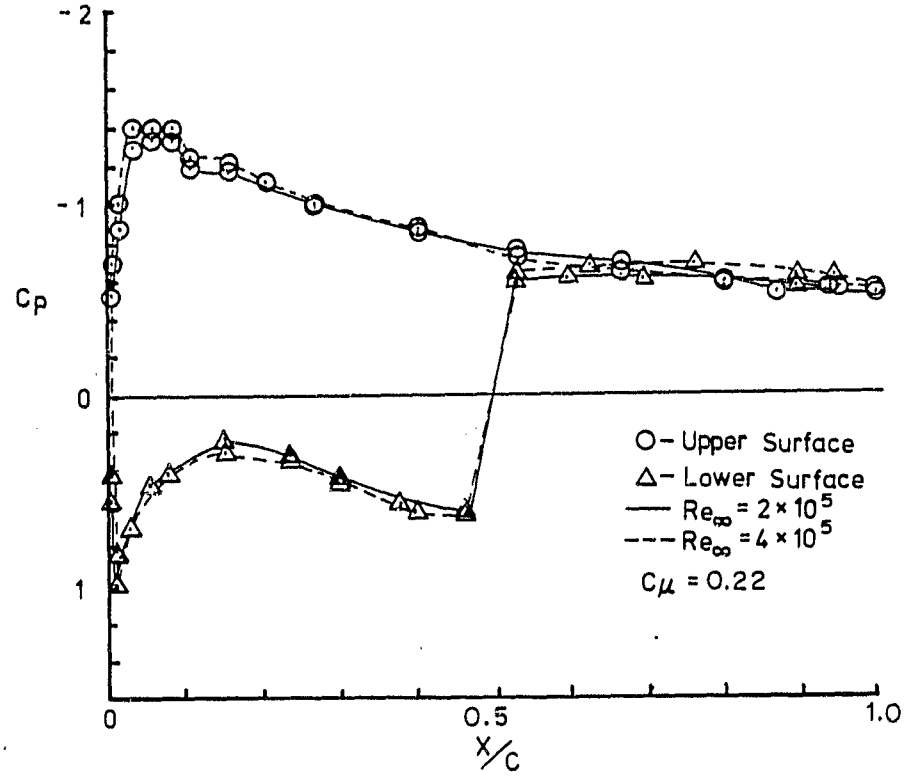

Figure 7. The distribution of the surface pressure on the airfoil at midspan and for two different free stream Reynolds numbers.

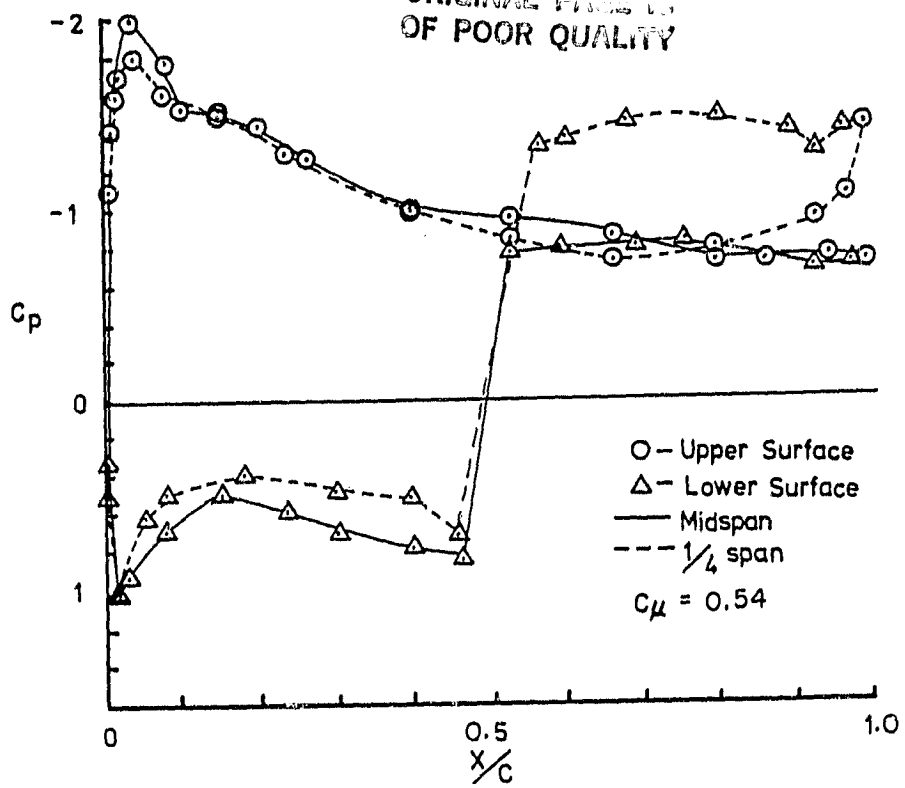

Figure 8. The distribution of the surface pressure at midspan and quarter span.

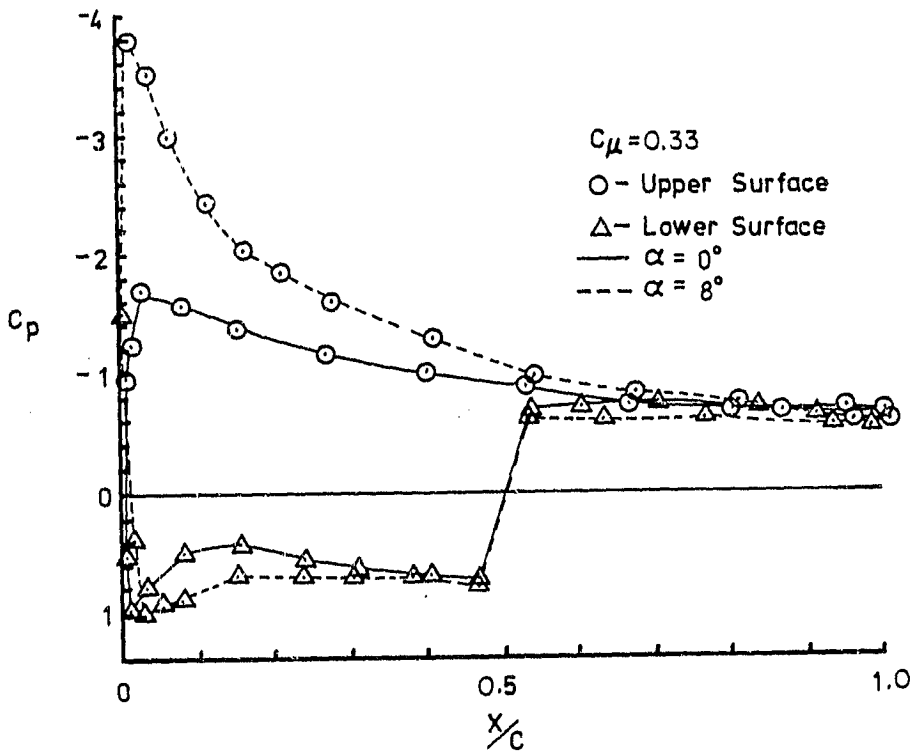

Figure 9. The distribution of the surface pressure at midspan for two different angles of attack.

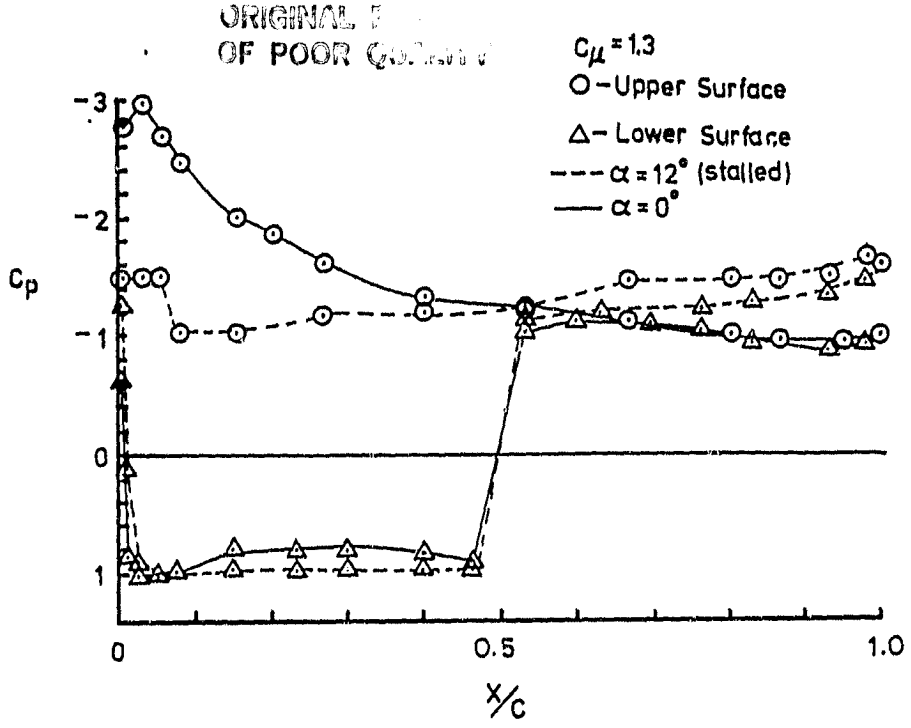

Figure 10. The distribution of the surface pressure at a post stall condition.

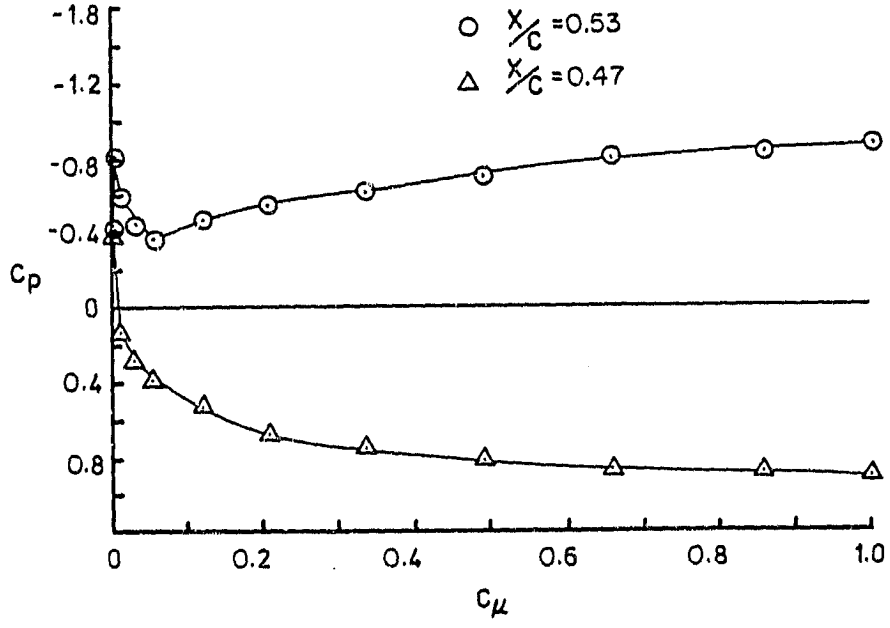

Figure 11. The variation of the surface pressure in front of and behind the jet with C_μ.

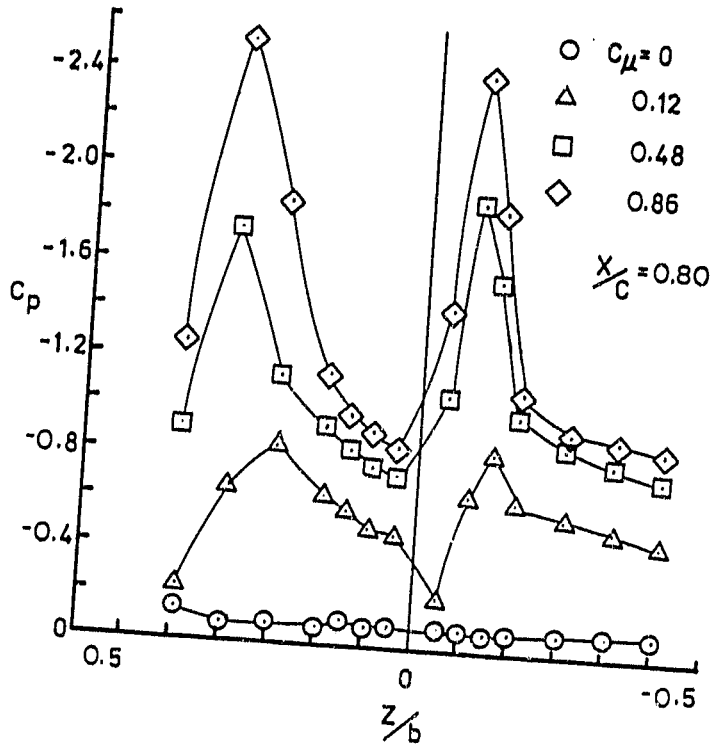

Figure 12. The distribution of the spanwise surface pressure behind the jet.

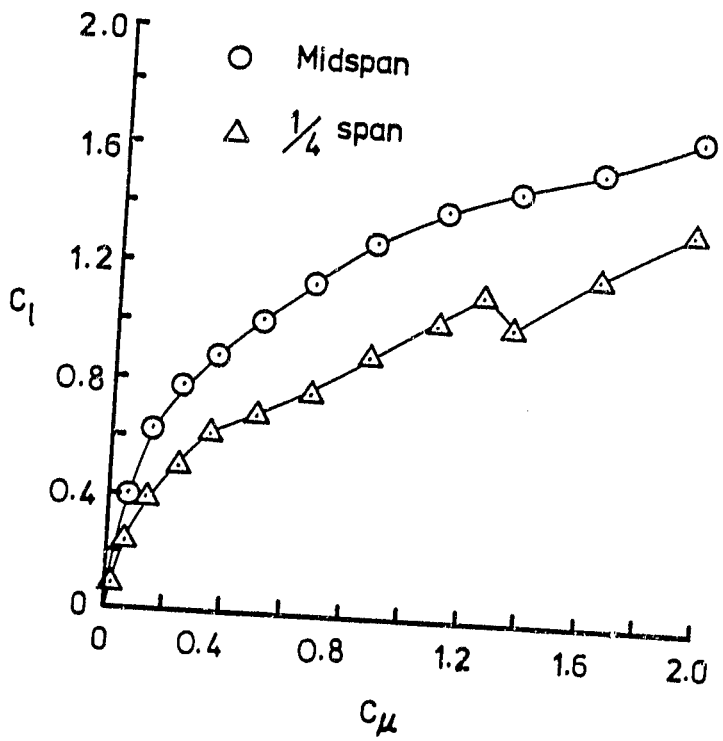

Figure 13. The variation of the sectional lift coefficient with C_μ.

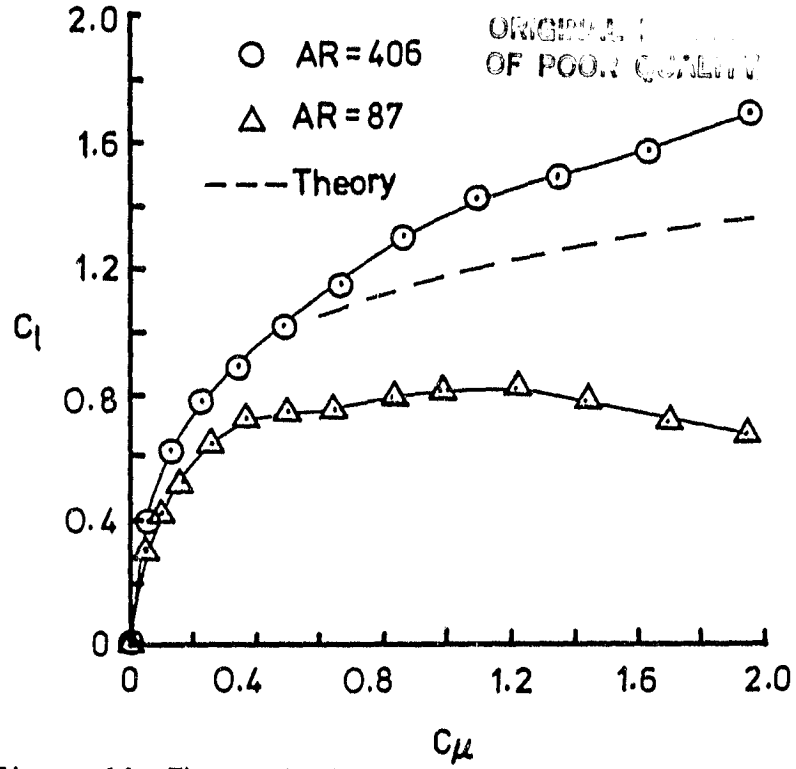

Figure 14. The variation of the sectional (midspan) lift coefficient with C_μ for two different aspect ratios of the nozzle.

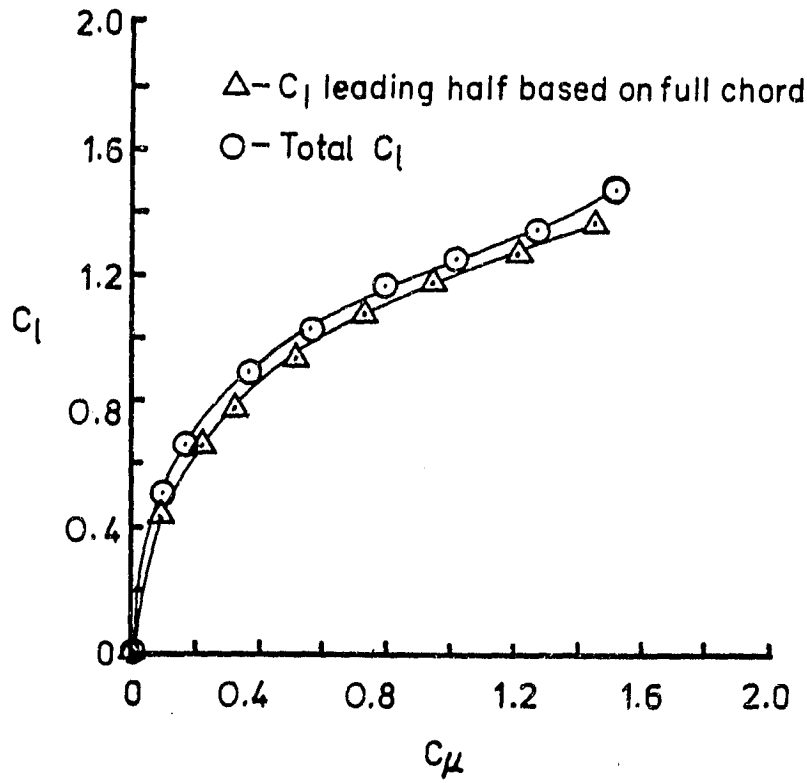

Figure 15. The variation of the sectional lift coefficient (midspan) with C_μ for the leading half of the airfoil.

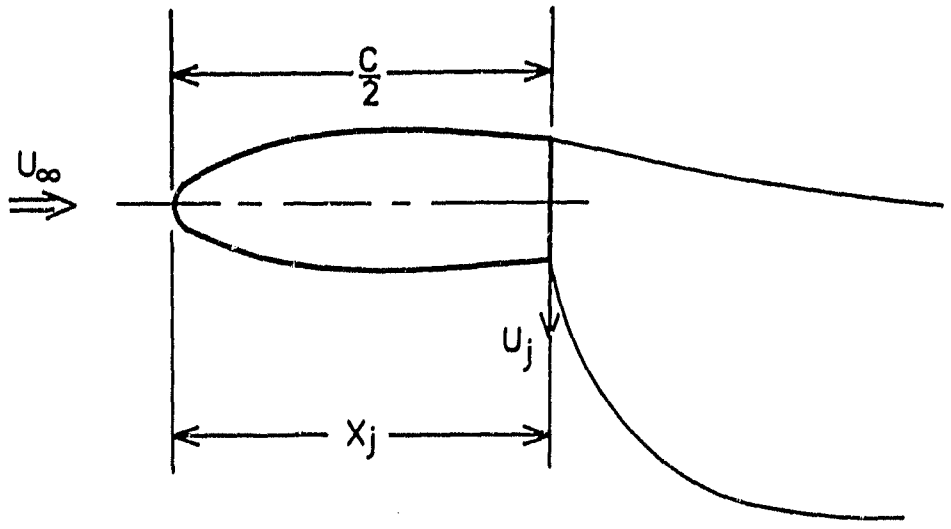

Figure 16. A schematic of the airfoil without the downstream half.

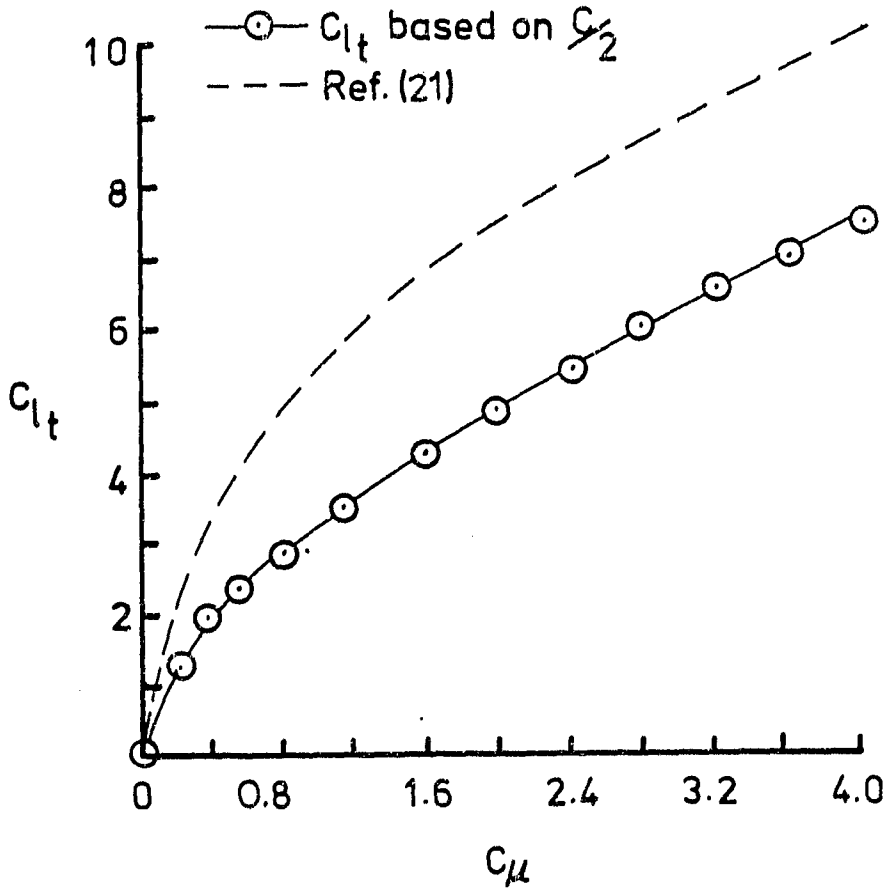

Figure 17. The variation of the sectional lift coefficient (midspan) with C_μ based on half chord length.

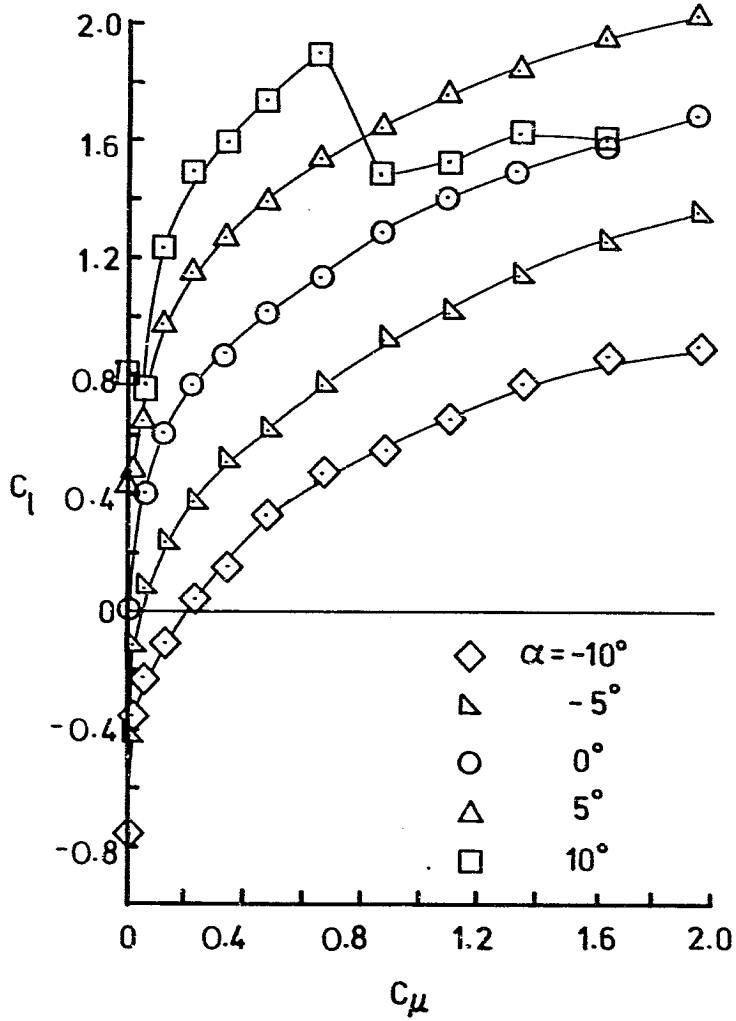

Figure 18. The variation of the sectional lift coefficient (midspan) with C_μ for different angles of attack.

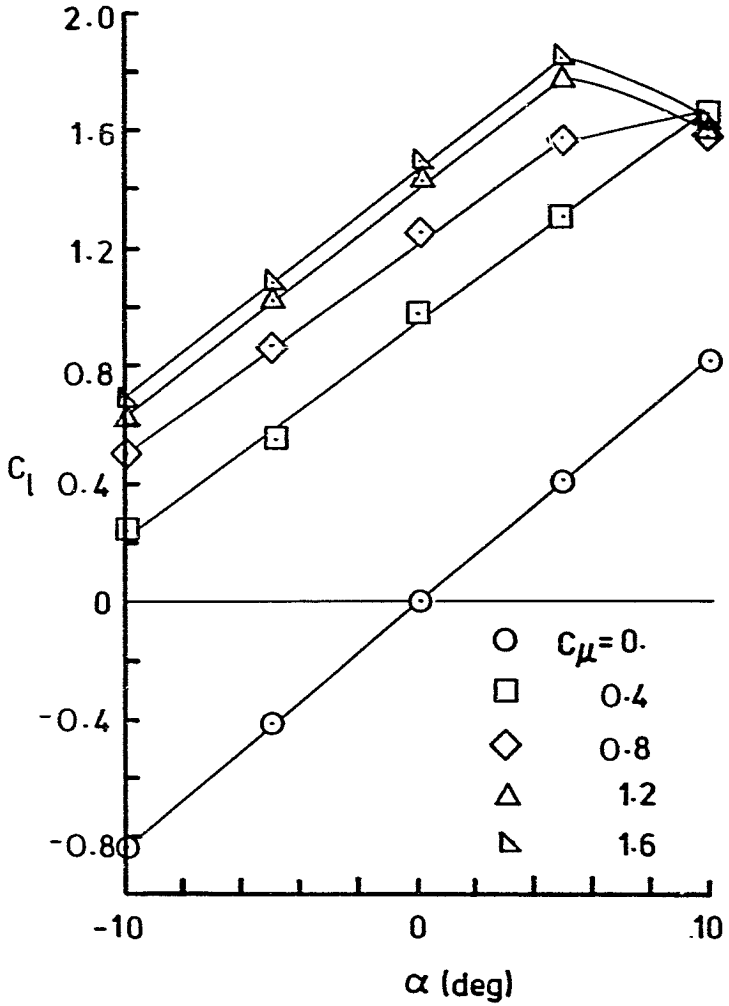

Figure 19. The variation of the sectional lift coefficient (midspan) with angle of attack for different C_μ.

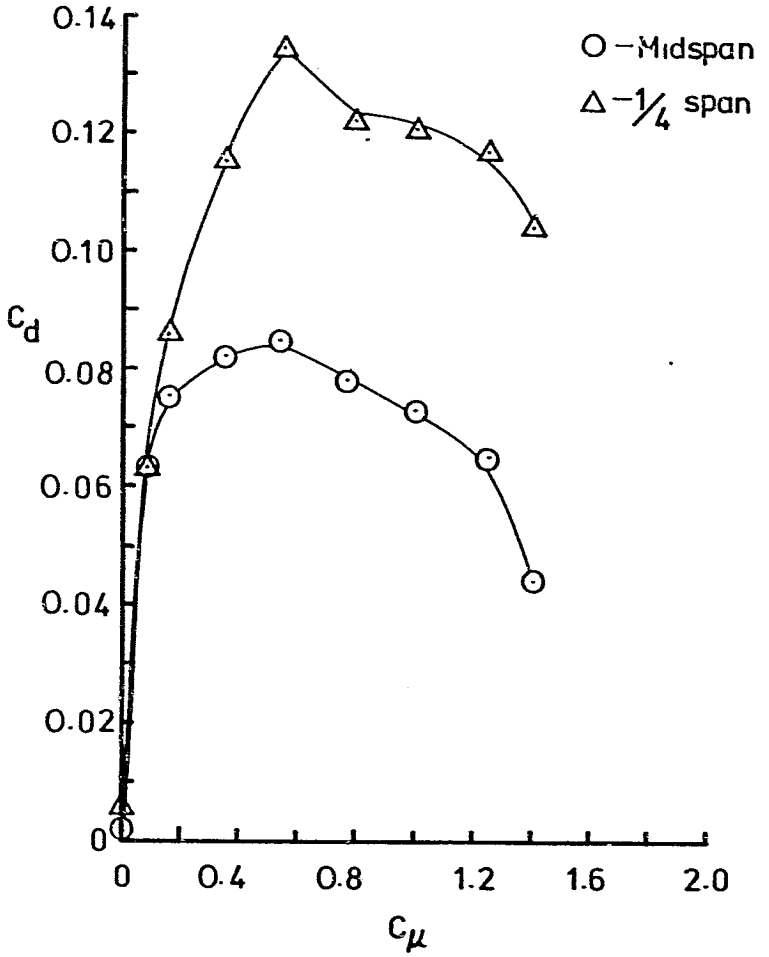

Figure 20. The variation of the sectional drag coefficient with C_μ at midspan and quarter span.

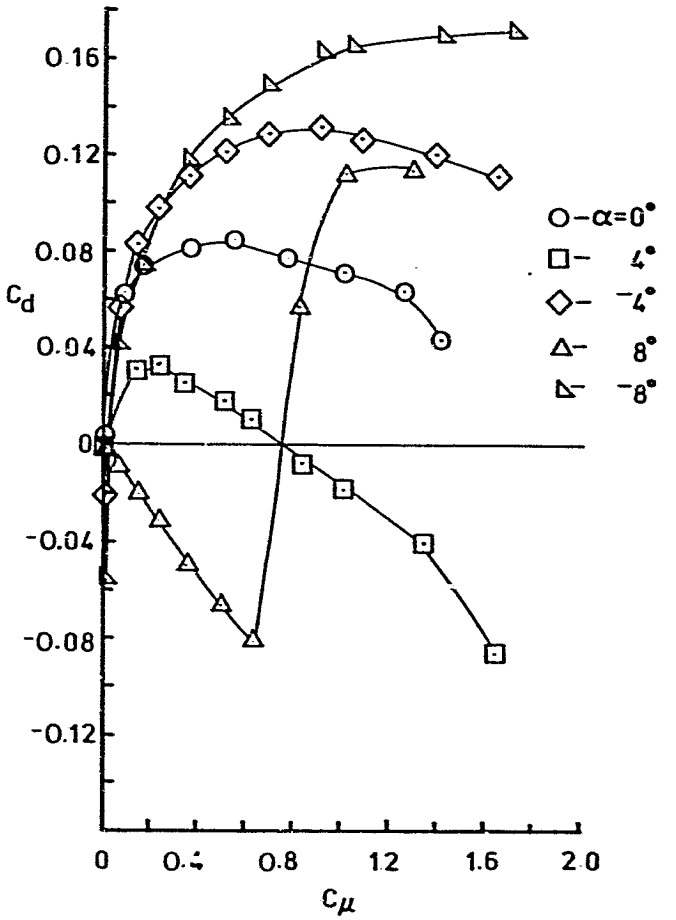

Figure 21. The variation of the sectional drag coefficient (midspan) with C_μ for different angles of attack.

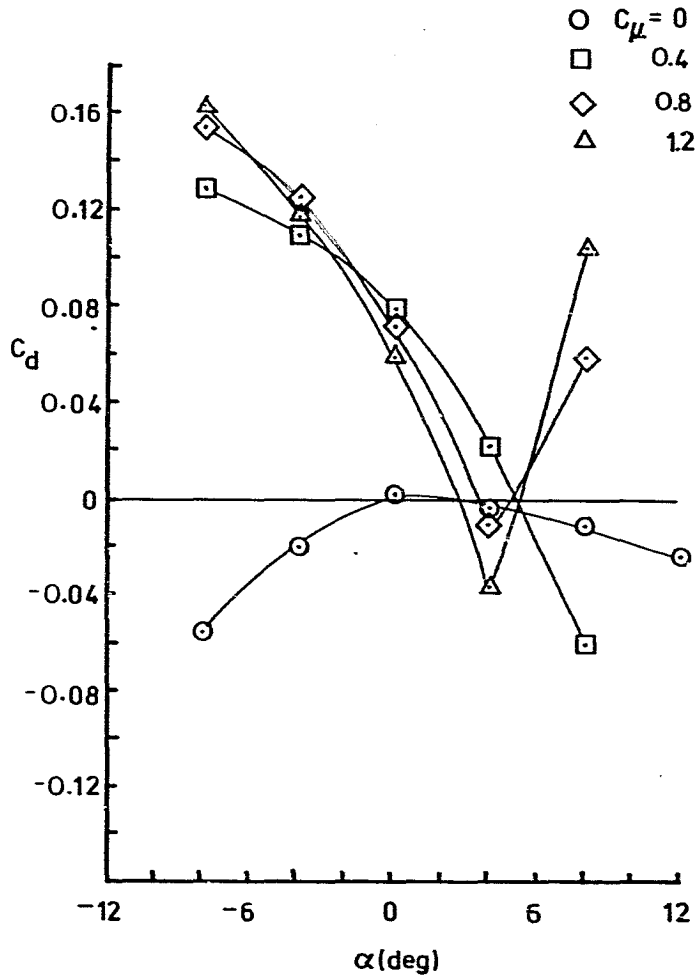

Figure 22. The variation of the sectional drag coefficient (midspan) with angle of attack for different C_μ.

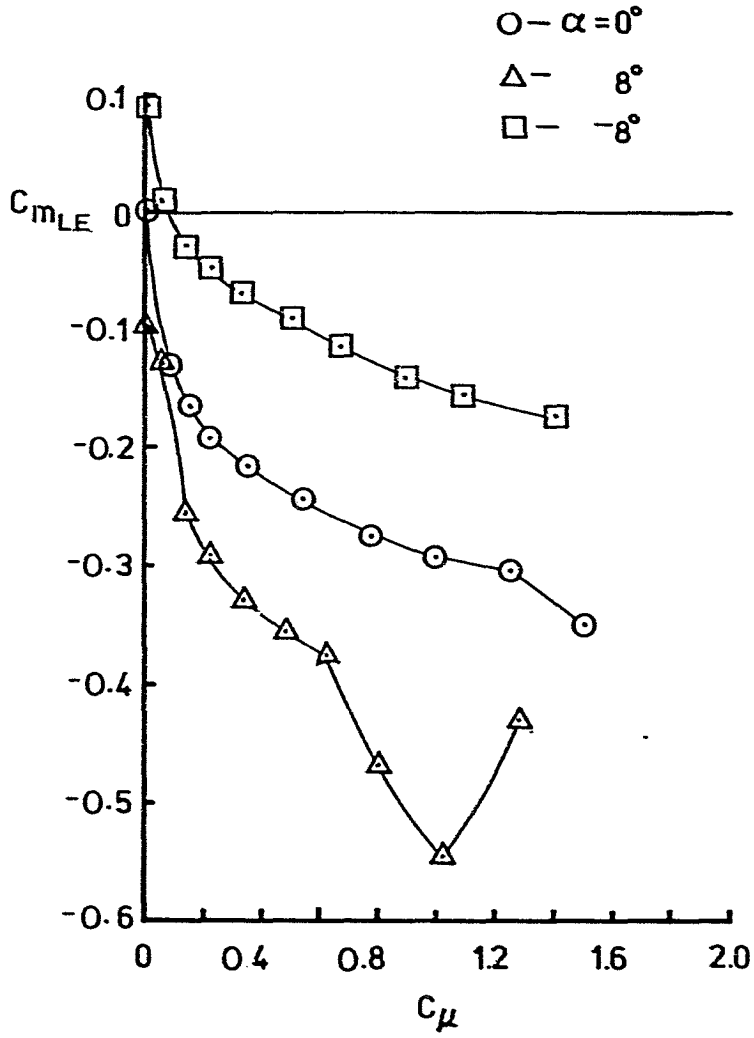

Figure 23. The variation of the moment coefficient at midspan with C_μ for different angle of attack.

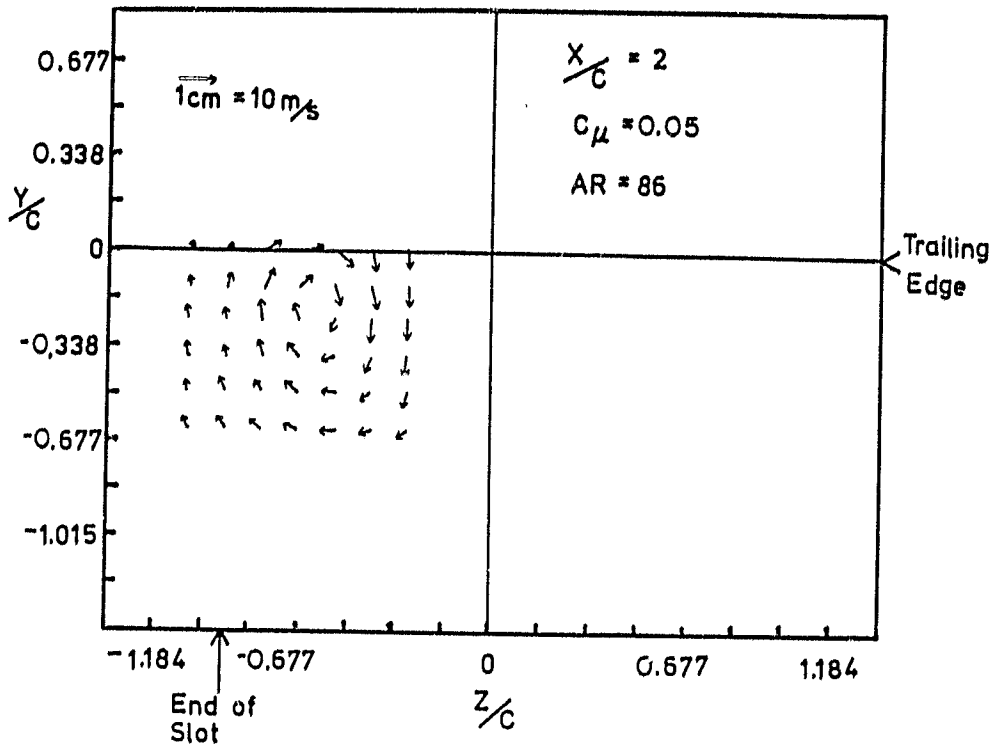

Figure 24. Velocity vectors in the Y-Z plane.

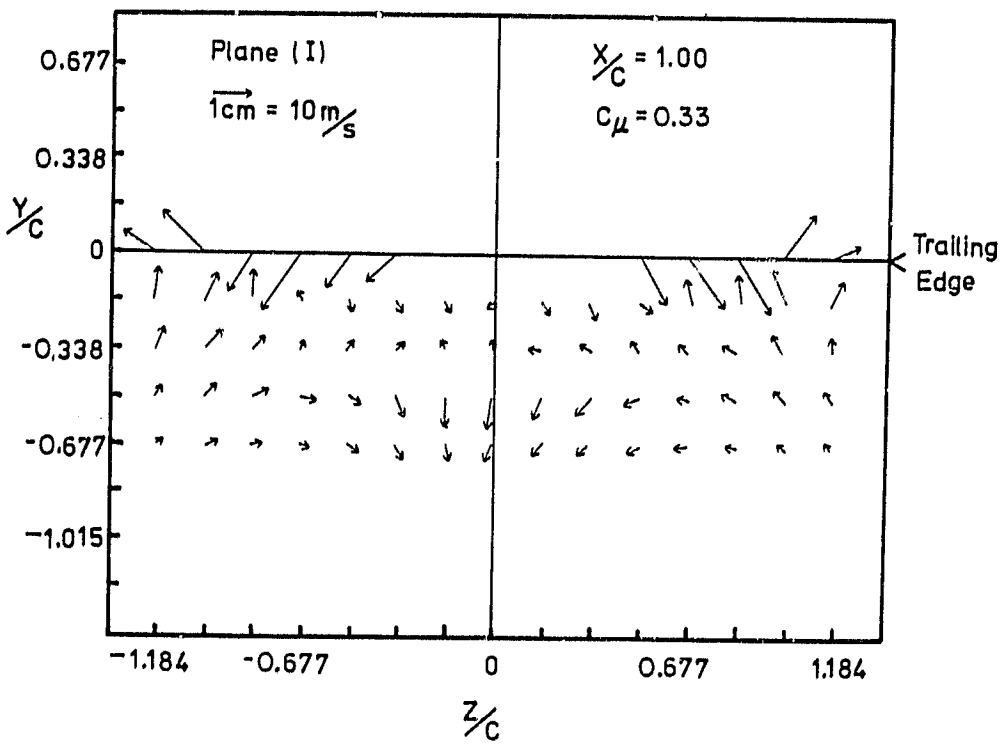

Figure 25. Velocity vectors in the Y-Z plane.

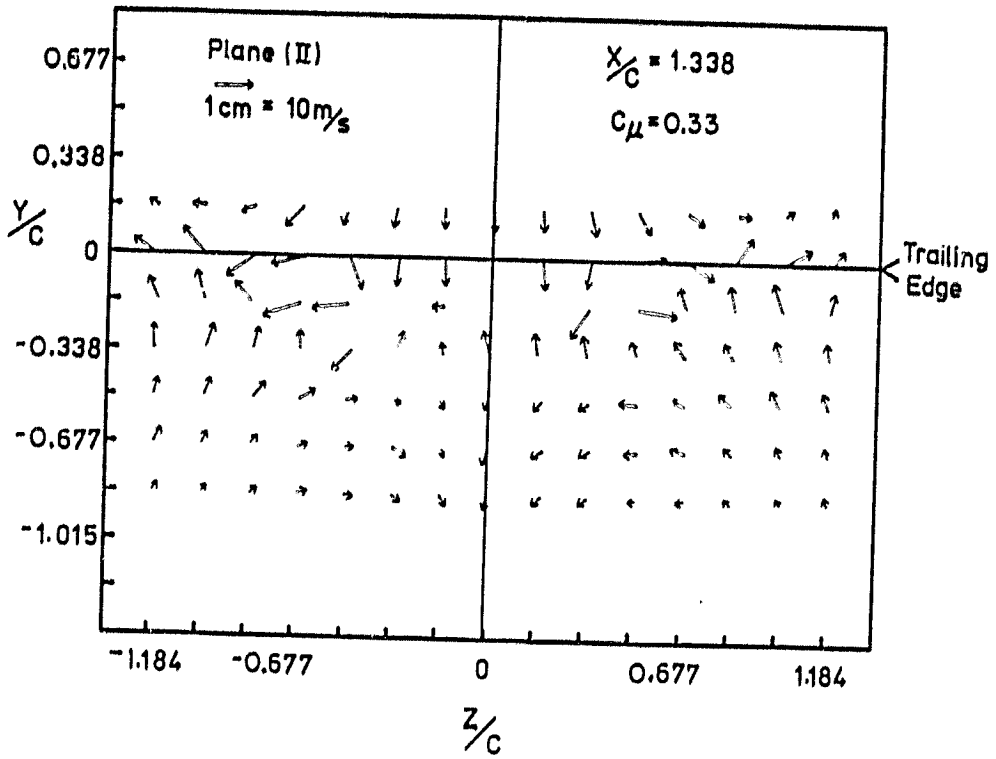

Figure 26. Velocity vectors in the Y-Z place for X/C =1.338.

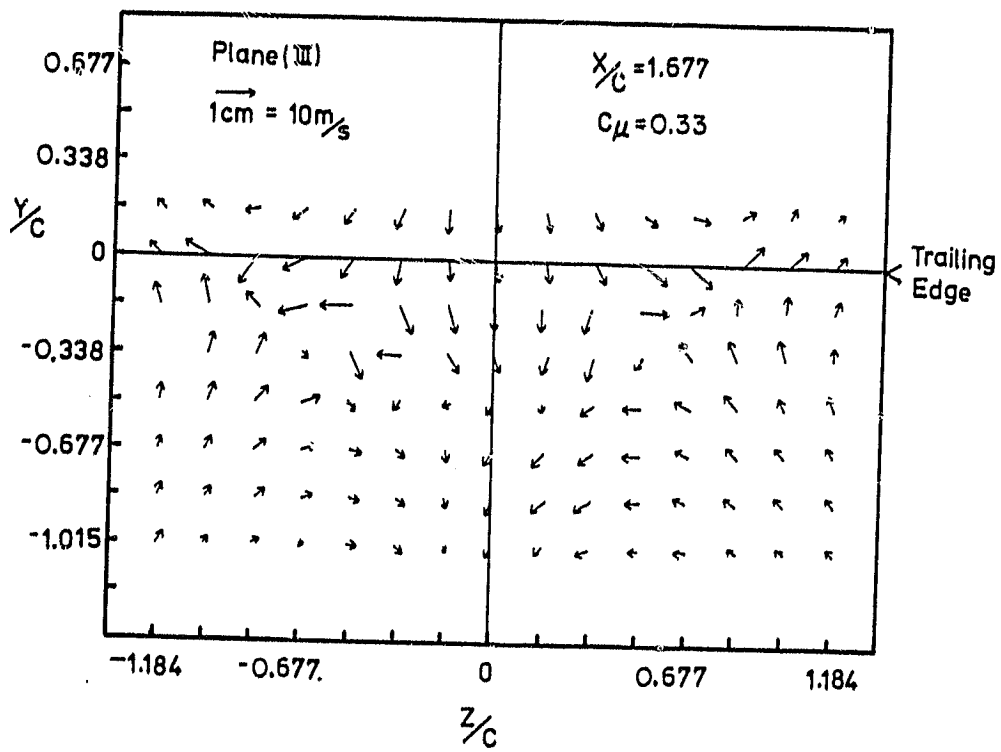

Figure 27. Velocity vectors in the Y-Z plane for X/C =1.677.

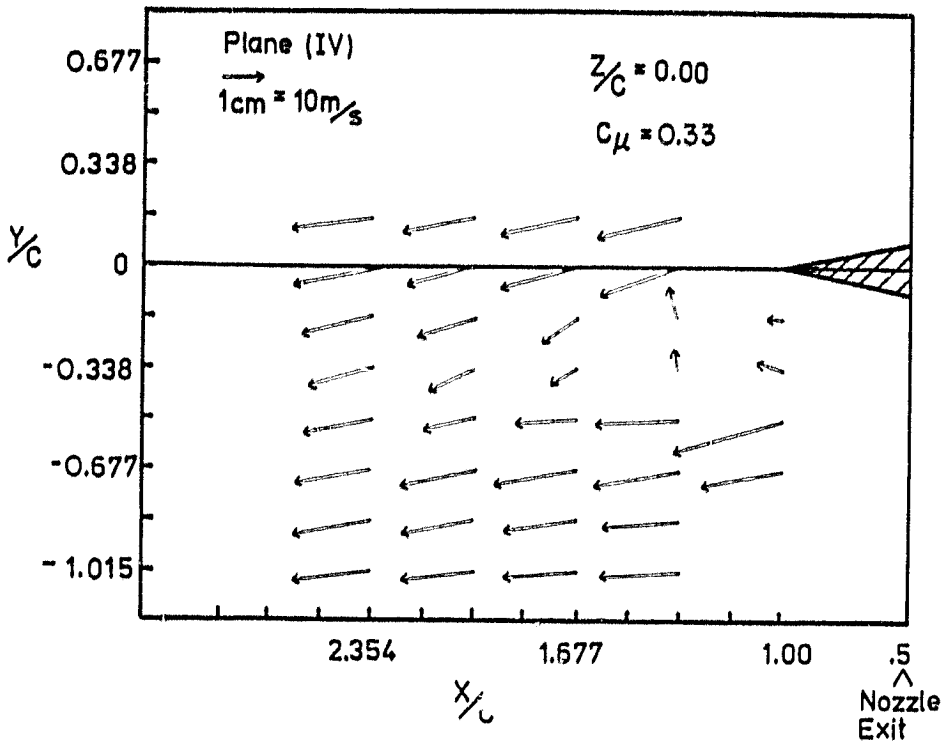

Figure 28. Velocity vectors in the X-Y plane.

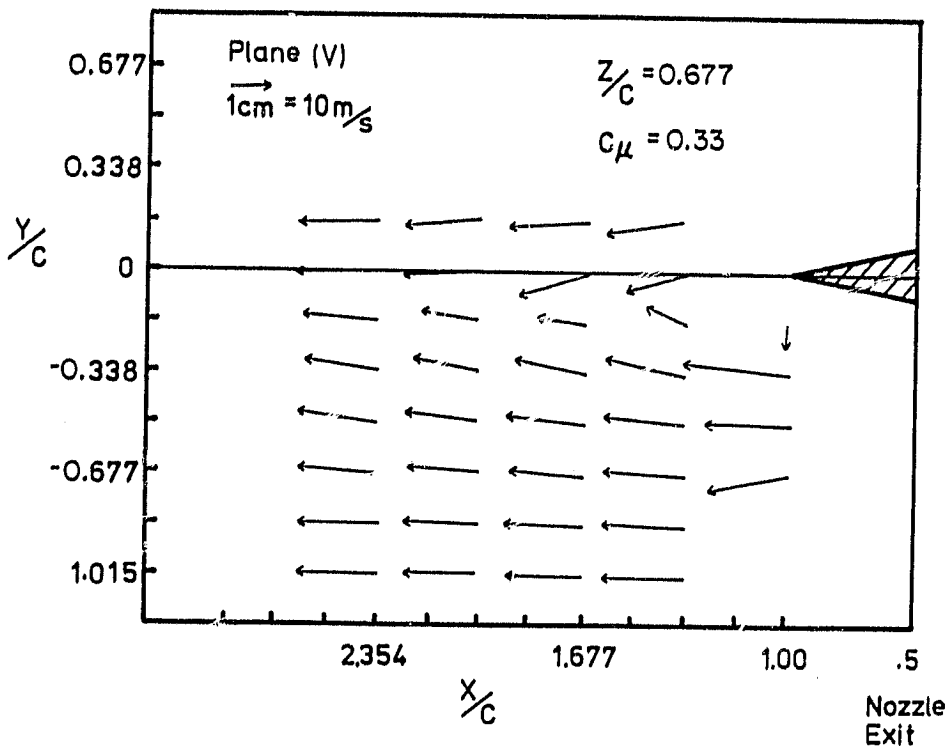

Figure 29. Velocity vectors in the X-Y place at Z/C =0.667.

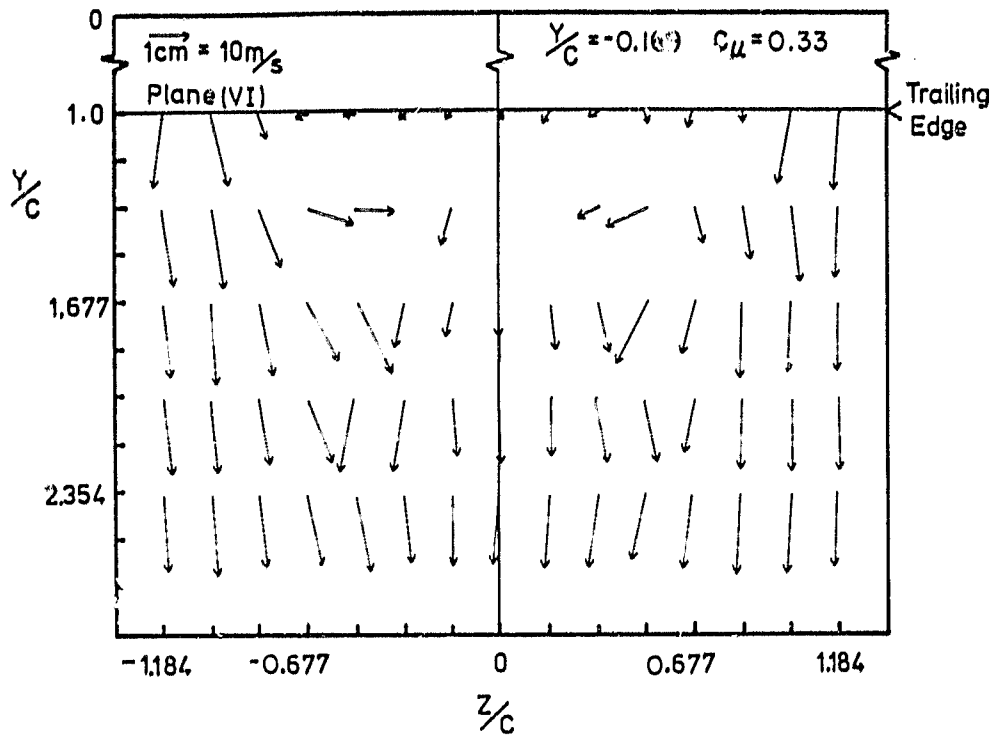

Figure 30. Velocity vectors in the X-Z plane at Y/C =-0.169.

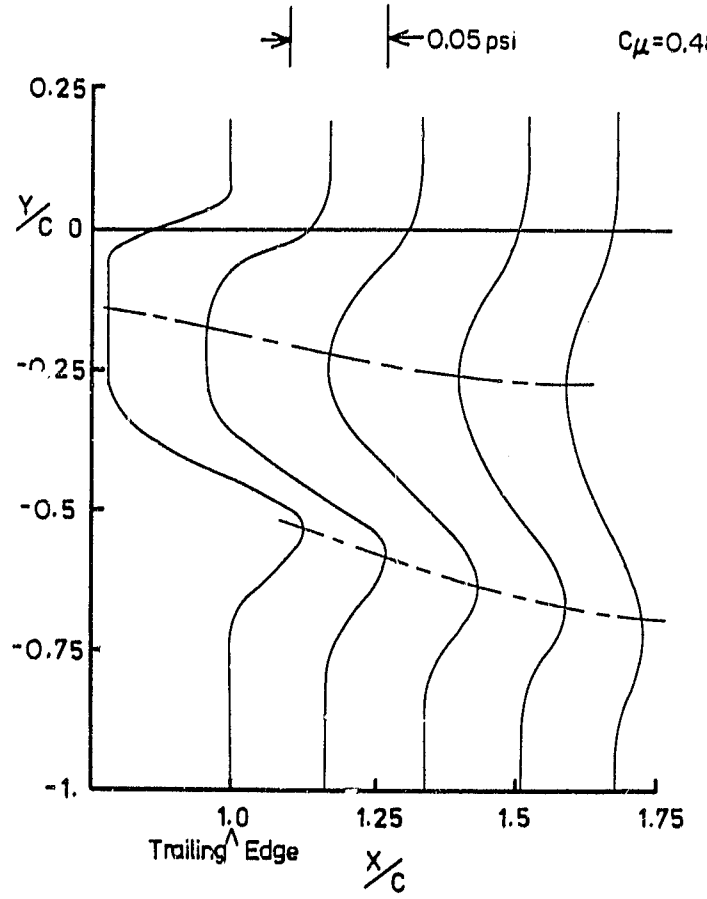

Figure 31. The distribution of the total pressure in the wake of the airfoil.

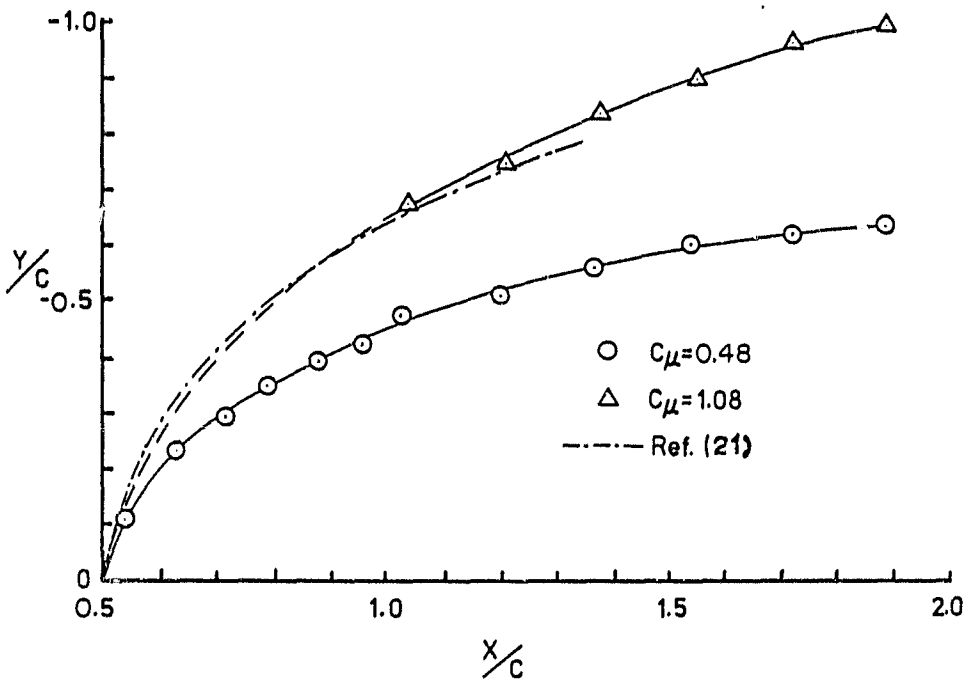

Figure 32. The location of the maximum velocity points in the jet with downstream distance.